Proc. Int. Symp. on Inverse Problems in Engineering Mechanics (ISIP 2001), 06-09 Feb 2001, Nagano, Japan
Elsevier Science, (2001)

USING THE GASDYNAMIC KNOWLEDGE BASE FOR AERODYNAMIC DESIGN AND OPTIMIZATION IN THE SONIC SPEED REGIME

M. TRENKER, H. SOBIECZKY
DLR German Aerospace Center
Bunsenstr. 10, D-37073 Göttingen, Germany

ABSTRACT

Refined concepts for high speed flow control in aerospace and turbomachinery applications suggest a retrospective look onto theoretical results of pre-CFD time for special airfoils, wings, bodies and internal flows because such results exhibit theoretically idealized behavior for some aspects in practical applications. Novel control mechanisms bring us closer to a mechanical realization of such special case studies. These provide known shape and (inviscid) flow properties in the transonic flow regime near Mach number unity, where numerical verification has always been a challenge to CFD and, for future generation SST concepts, an application to swept wings in supersonic flow.

KEYWORDS

Transonics, Supersonic transport, SST, Airfoils, Swept wings, Inverse design, Hodograph solutions, Shock waves

INTRODUCTION

In a recent workshop on supersonic transport concepts [1] the present status of aerodynamic design methodology was reviewed and several topics were shown to be a special challenge to CFD as well as to the development of optimization strategies for achieving desirable aerodynamic performance. Recently developed methods for this goal include inverse approaches as well as the simulation of genetic (evolutionary) optimization. In this situation of having arrived at efficient computerized design it seems worthwhile to recollect the knowledge bases in fluid physics and theoretical aerodynamics, to select known case studies for a practical verification by new algorithms or even for a realization by novel mechanical concepts like variable geometry components for adaptation in varying operating conditions.
In this contribution analytical results for transonic airfoil flows based on exact mathematical (hodograph) models are chosen as special test cases which can be defined also by a general configuration definition geometry preprocessor. Slender analytical airfoil flows with known lift,

wave drag and pressure distribution are sought to serve as baseline wing sections, first for CFD code validation and subsequently by shape parameter variations to study thin supersonic swept wings with predefined accelerated flow pressure distributions, which may be found useful for viscous flow control.
Layout of control surfaces for adaptive configurations like nose droop and sealed flaps and slats for transonic applications and high speed wings profits from the existence of such special solutions and their CFD verification.
Also, approach of supersonic Mach numbers to $Mach_\infty \rightarrow 1$ carries the difficult problem of simulating numerically or measuring experimentally a sonic boom, i. e. the detached shock wave in front of the airfoil: CFD grid resolution as well as wind tunnel far field conditions simulation hardly are suitable for observing a precise wave strength and location. Transonic inverse design including input shock wave (sonic boom) modelling may profit from analytic relations for the location, geometry and strength of the detached bow wave.

NEAR SONIC FLOW

No other phenomena within the world of inviscid compressible flow have challenged the pioneers of gasdynamics, CFD and applied aerodynamics to such an extent as those involving transonic flow: The mathematically interesting co-existence of elliptic and hyperbolic basic differential equations led together classical methods of hydraulics with those of wave propagation, with mixed boundary/initial value problems in 2D and in 3D space. For inviscid flow simplifications this has led to a couple of model solutions, the most well-known of which is the accelerated flow through a Laval nozzle. About 3 decades ago, the second author was able to extend some of this theoretical ‘knowledge base’ models to aerodynamically relevant test cases for numerical simulation (CFD) which by then was just starting to be a new field of fluid mechanics.
After CFD having become a strong and useful tool for almost every aerodynamic problem, these model solutions may still serve for some validation purpose because they offer a complete description of a flow field including the velocity or pressure distribution around an aerodynamic 2D airfoil or body of revolution. Parametric representations for ***flow geometry*** as well as ***flow quality*** are given as closed form solutions [2], (see Fig. 1). For a recent presentation with new applications see [3].

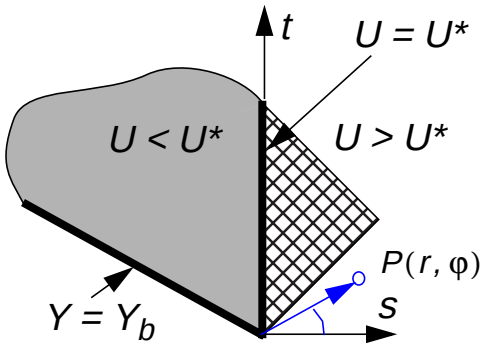

$$U = r^n \cdot h(\varphi)$$

$$V = r^{n + p_1 \cdot b} \cdot k(\varphi)$$

$$X = r^{b + p_2 \cdot n} \cdot f(\varphi)$$

$$Y = r^b \cdot g(\varphi)$$

Figure 1. Parametric representation (s, t) of flows by their quality (velocity components U, V) and their geometry (X, Y), observing boundary conditions (Y_b) and type change of the basic equations of motion at the sonic line (U = U*). See ref [3].

Moreover, novel concepts of flow control using sophisticated mechanic devices are under development now and we are willing to achieve special goals which are defined by ‘target functions’ for pressure and other specific details of the flow structure. In this situation we remember that some quite ideal flows are modeled by those solutions in a closed analytical form. In the present contribution we want to alert the design aerodynamicist on some of these solutions for a slender airfoil with variable camber, as a baseline geometry for lifting wings in transonic or supersonic flow.

Airfoils in Mach ≥ 1

Without going into any of the details leading to these hodograph (“Rheograph”) solutions, we give here the most relevant formulae defining the variable camber airfoil and its pressure distribution in a uniform sonic flow ($M_\infty = 1$).

Thickness to chord ratio is depicted by τ and camber to chord ratio by ω (see Fig 2). The solution is exact for $\tau \to 0$ and practically valid for slender airfoils ($\tau < 0.1$), and includes a symmetrical airfoil ($\omega = 0$, known as “Guderley’s cusp”) but also cambered wing sections with a ratio ω/τ up to 0.5. With parameter $p(\omega/\tau)$ defined by (1),

$$p = p\left(\frac{\omega}{\tau}\right) = 2^{13/2}3^{3/2}5^{-7/2}\frac{\omega}{\tau}\left(1 + 2^{12}\cdot 3\cdot 5^{-6}\left(\frac{\omega}{\tau}\right)^2\right)^{-1/2} \qquad \text{(Eq. 1)}$$

the family of cambered airfoils is given by (2):

$$y_p(X) = \tau\cdot X(1-X)\left(2^2\cdot\frac{\omega}{\tau}\pm 2^{-2}\cdot 3^{-3/2}\cdot 5^{5/2}\cdot X^{1/2}\right) \quad . \qquad \text{(Eq. 2)}$$

The cusp is pointing into the flow so that it is smoothly passed by the stream without the flow forced around the sharp leading edge; this results in the definition of an angle of attack of the flow (or the airfoil), (3):

$$\alpha = \tau\cdot 2^{-9/2}3^{-1/2}\cdot 5^{5/2}p\cdot\frac{1-2^{-1}3^{-4}5\cdot 13p^2}{(1-2^{-1}3^{-2}5p^2)^{3/2}} \qquad \text{(Eq. 3)}$$

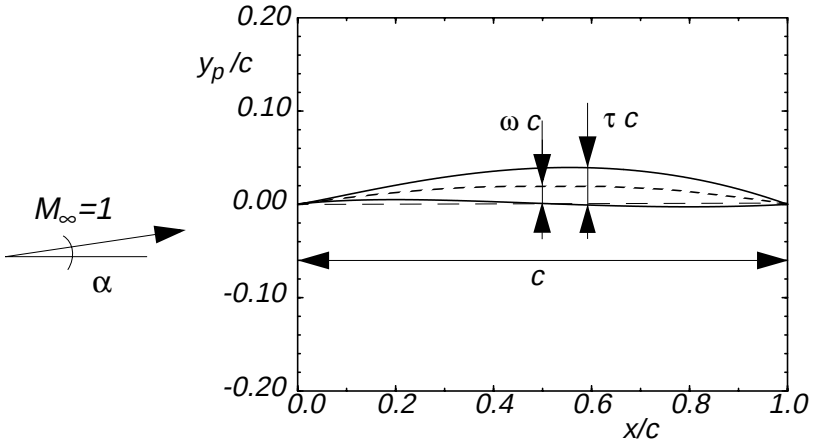

Figure 2. Cusped airfoil with prescribed angle of attack in sonic freestream. Drawn airfoil has camber/thickness ratio 0.5

Aerodynamic coefficients

The sharp leading edge (of a 3D wing with this 2D cusped airfoil) in sonic freestream ($M_\infty = 1$, α) results in a smooth pressure distribution without a stagnation point, (4):

$$c_p = \frac{(5^2 \cdot \tau)^{2/3}}{(2^2 \cdot 3 \cdot (\gamma+1))^{1/3}} \left[\frac{(1 - 2^{-2}3^{-2}5p^2)}{(1 - 2^{-1}3^{-2}5p^2)} - 2^{-1}5X \mp \frac{2^{-1/2}3^{-1}5p \cdot X^{1/2}}{(1 - 2^{-1}3^{-2}5p^2)^{1/2}} \right] \qquad \text{(Eq. 4)}$$

This pressure distribution can easily be integrated to result in lift and drag components which are depicted in Fig. 2 for all relevant camber/thickness ratios $0 < \omega/\tau < 0.5$. Given an adjustment of the respective angle of attack $\alpha(\omega/\tau)$ according to (3) we obtain the drag polar for an adaptive wing section in sonic flow, modeling a flexible airfoil of given thickness bent to variable camber.

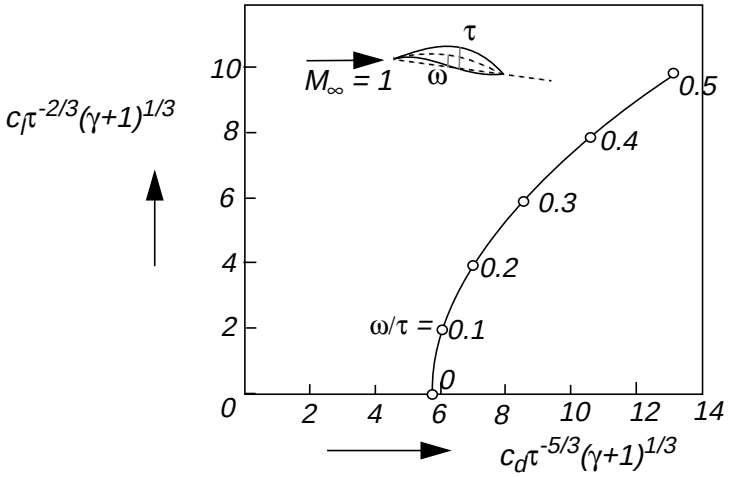

Figure 3. Lift and drag coefficients for an airfoil with variable camber in sonic flow conditions

Detached bow wave

With the flow quality and airfoil geometry for this cusped slender airfoil being completely defined in sonic freestream, we also have results for the approach of a detached shock wave once the Mach number exceeds unity: A similarity solution for this flow was obtained [4], explaining the shape, strength and location of a detached shock wave for varying Mach numbers slightly above $M_\infty = 1$. An asymptotic mapping of the bow wave into a universal image including escape of the shock if $M_\infty \to 1$ is depicted in Fig. 4: We see that the physical coordinates (x,y) are obtained from stretching the image (X,Y) if the Mach number approaches unity. Such bow waves are neither easily simulated numerically, nor can they be measured in a wind tunnel or even using flight tests. The model solution can therefore serve the development of improved numerical techniques.

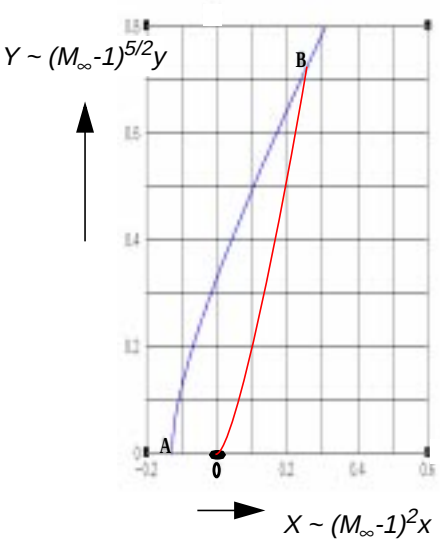

Figure 4. Detached bow wave (AB) and sonic line (OB) resulting from an airfoil in slightly supersonic flow: Similarity solution

Bow wave attachment

Once the transonic Mach number M_∞ is high enough the flow will attach to an airfoil with sharp or wedge leading edge. This process is still interesting from the need of better understanding the local flow quality at the leading edge: A change from the normal ("strong solution") shock of the detached bow wave to the oblique "weak solution" shock is modelled by a local flow pattern with a weak singularity which affects the pressure distribution at the wedge nose:
Shock attachment results in a pressure distribution modeled by (5)

$$c_p = a + \frac{b}{\log x} + c \cdot x^d + \ldots\ldots \qquad \text{(Eq. 5)}$$

with a, b, c and d being functions of the Mach number; the logarithmic term occurring only when the flow attaches ($M = M_{attach}$), while power d starting from zero at this condition, reaching 1 at the so-called Crocco point ($M = M_{Crocco}$) and rising to higher order until the attached flow post shock condition passes sonic and enters supersonic conditions at $M = M_{upcr}$). Fig. 5 shows this qualitatively, a more detailed report [5] illustrates the method to analyze such flow details with the hodograph transformation and conformal mapping. This detail may be academic, but it could be of interest for the definition of properly posed boundary conditions defined from prescribed target functions in inverse design and optimization.

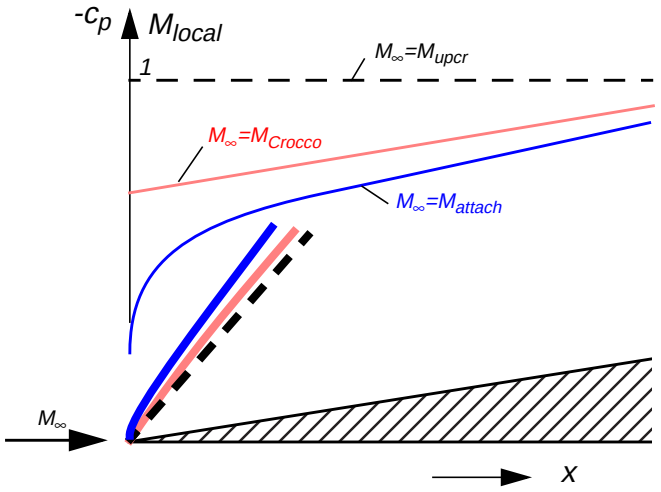

Figure 5. Pressure distribution or local Mach number (qualitatively) for wedge flow in supersonic Mach numbers between shock attachment and completely supersonic post shock conditions.

GEOMETRY GENERATION

Inverse design and optimization may be well advised to observe certain details in the boundary conditions of given or desired shapes and target functions. The above local phenomena may serve as test cases to obtain very special cases but if a design strategy is well able to verify results with these details then it can be trusted for solving problems with more average case studies.
Prescribing model functions for 2D airfoils and 3D wings as well as target pressure distributions with suitable parameters should therefore include these details, among the more practical shapes of subsonic and purely supersonic flow geometry and quality. The PARSEC family of airfoils and pressure distributions is illustrated in another contribution [6], we have defined its parameters in a way that the abovementioned cusped shapes and transonic flow phenomena are included

in its posible case studies. Refined flow control techniques like adaptive nose drooping for novel helicopter airfoil improvements [7] could, in principle, also be applied to high speed configurations with sharp, cambered leading edges, the presented exact solutions might serve for numerical design efforts.

Airfoils and wings

Fig. 6 illustrates the geometry of a presently interesting case study: An oblique flying wing (OFW) for transonic and supersonic transport is defined by cusped slender airfoils as described in (3), with camber and wing twist defined as functions of the wing spanwise direction, to be varied in inverse design or optimization strategies.

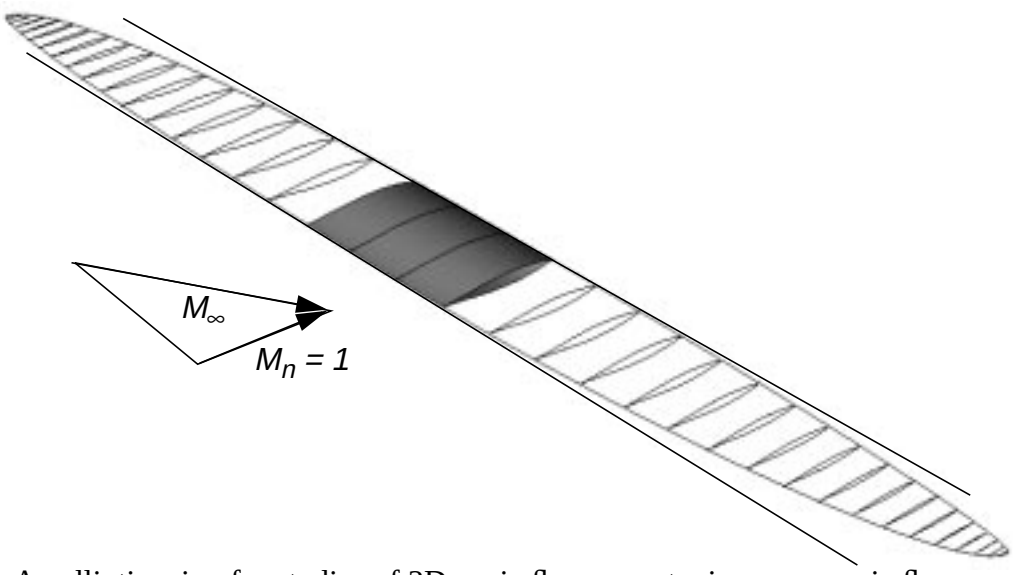

Figure 6. An elliptic wing for studies of 2D sonic flow, swept wing supersonic flow and fully 3D supersonic wing flow with optimum aerodynamic performance. Analytical surface geometry generation using variable camber cusped airfoils.

NUMERICAL SIMULATION EXAMPLES

This presentation is basically illustrating models which could be of use for CFD with highly efficient and accurate numerical flow codes, to be used in Euler (inviscid) mode first for verifying theoretically advised input data, which subsequently may prove favorable when the viscous effects of real flow conditions are taken in account with Navier-Stokes versions of such codes. The following few examples illustrate an approach to use an unstructured grid solver (DLR-τ), [8], with solution - adaptive grid refinement which may be driven toward a very precise representation of the abovementioned special airfoil flows and singularities accompanying transonic shock waves. For viscous flow the code works with hybrid grids with structured layers near the surface boundary conditions, here we so far use only the unstructured option for inviscid flow.

Airfoils in sonic freestream flow

Guderley's and the cambered cusped airfoils defined by (1), (2) and (3) in Mach number unity flow are among our first results, see Fig. 7. Grids with 36000 points show already a satisfactory representation of the expected pressure distribution (4): The linear distribution for the symmetrical Guderley cusp and a linear plus superimposed square root model for the cambered lifting section.

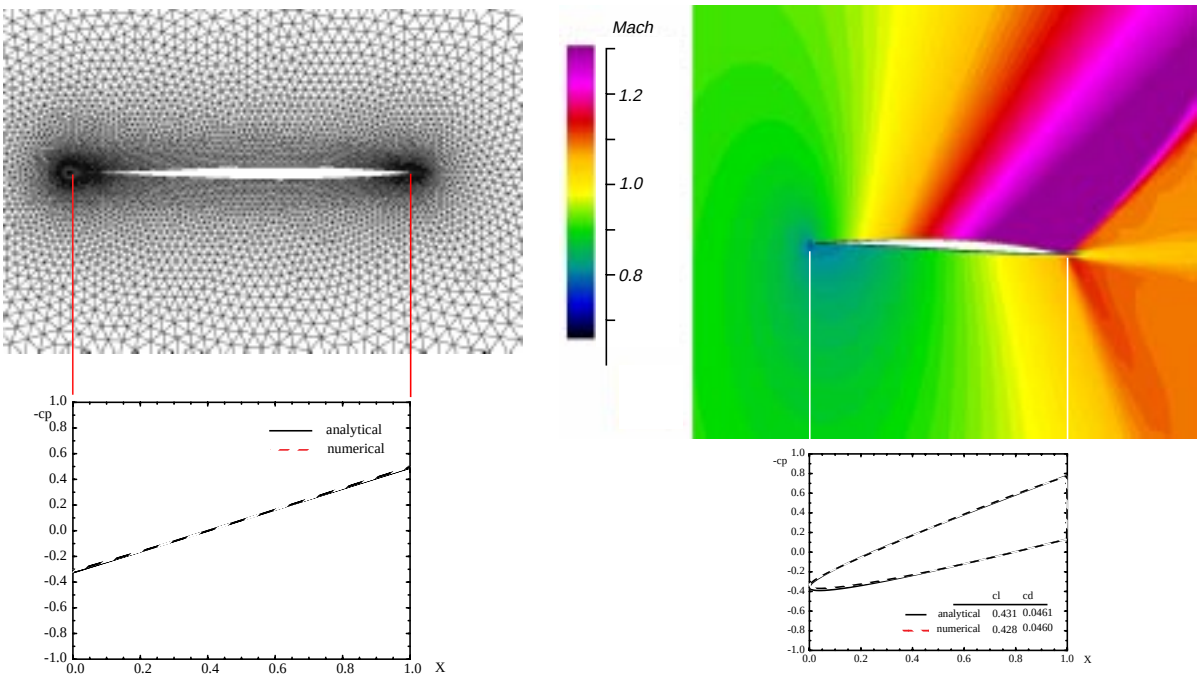

Figure 7. Symmetrical and cambered cusped airfoils in sonic freestream conditions: Grid and linear pressure distribution for Guderley's cusp (a), Mach number isofringes and pressure distribution for lifting airfoil (b); comparison of analytical and numerical results

Simulation of a detached bow wave

Airfoils in slightly supersonic freestream conditions create detached bow waves which usually are not represented well in numerical simulation because of too coarse grids in the flow field off the airfoil. Our results obtained from using the DLR-τ code are illustrated in Fig. 8. They show the code option of local grid refinement where steep gradients are detected in the flow field. We use these computational solutions for various Mach numbers slightly above unity to check the practical validity range of the similarity solution shown in Fig 4:
The stand-off distance of the shock wave from the leading edge with its asymptotic behavior for $M_\infty \rightarrow 1$ was checked and for some Mach numbers depicted in the diagram in Fig 8.
Such computations may be useful when analytical results for far field sonic boom propagation need to be fitted with local flow field results including aircraft geometry.

Simulation of bow wave attachment

Numerical studies with bow wave attachment were carried out in order to observe the analytically predicted behavior to a degree which results from practical grid refinement options of the DLR-τ code. A double wedge (diamond) airfoil was used for these computations. Here only the interaction of the leading edge with the bow wave is of interest; (the wedge shoulder creates another locally singular flow behavior). The results obtained for Mach numbers close to attachment conditions are illustrated in Fig. 9, so far the are used to gain confidence in CFD data for local pressure distributions affecting viscous effects like transition modelling at the leading edge.

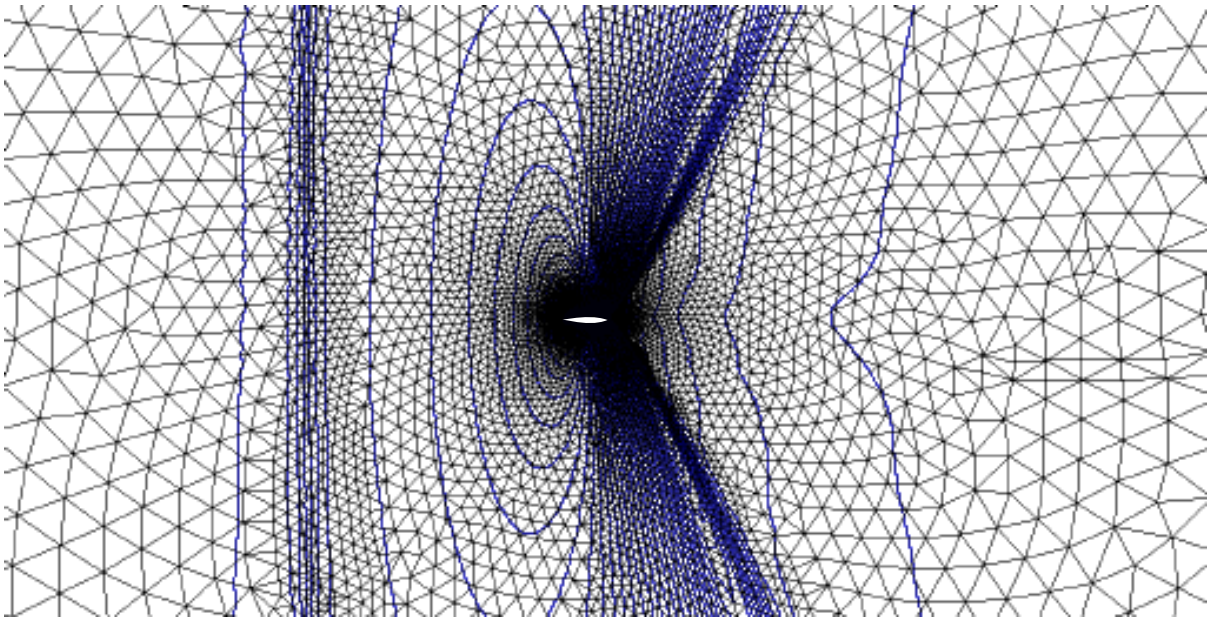

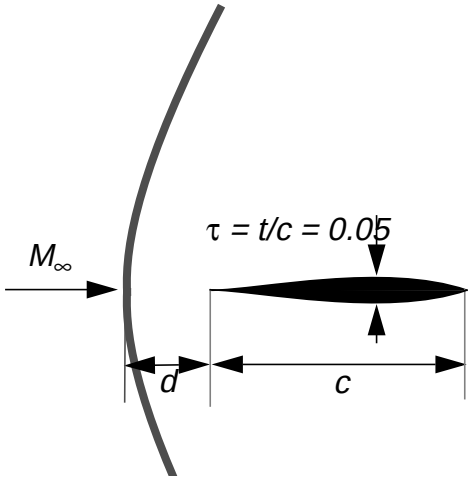

M_∞	d/c
1.024	6.2
1.059	1.0
1.092	0.23

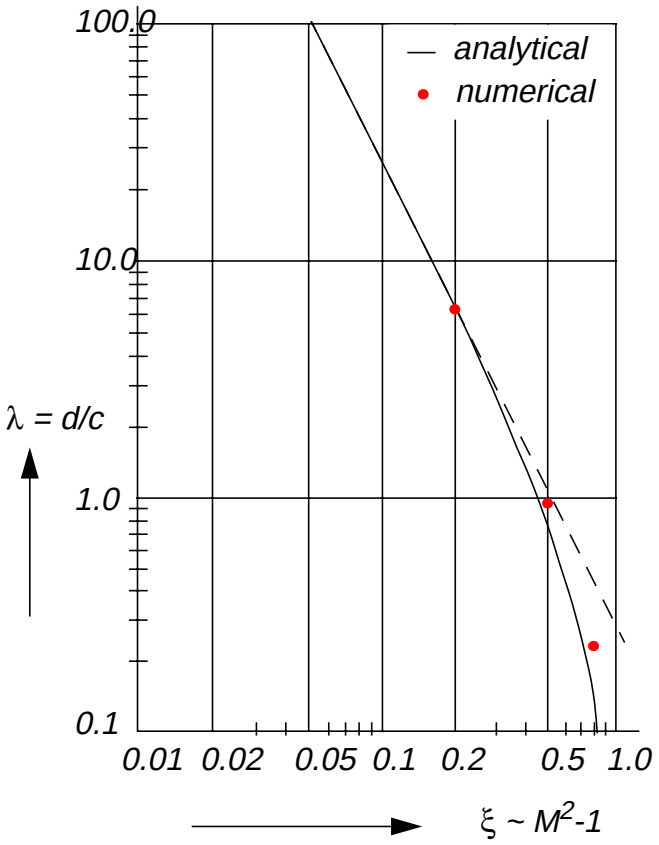

Figure 8. Numerical simulation of a detached bow wave in front of a Guderley cusp using the DLR -τ code: Grid segment with local refinements near airfoil and where steep gradients (shocks) occur. Three Mach numbers computed, comparison of stand-off distance with analytical hodograph solution [5].

$M_\infty = 1.1178$ $M_\infty = 1.1244$ $M_\infty = 1.1309$

$d/c = 0.0175$ $d/c = 0.0045 \sim 0$

Figure 9. Isofringes illustrating the process of shock wave attachment: Normal strong shock turns to oplique weak shock when attachment takes place. (Here: wedge nose of diamond airfoil, $\tau = 0.05$, shock stand-off distance d/c vanishing at $M_\infty = M_{attach} \sim 1.1244$

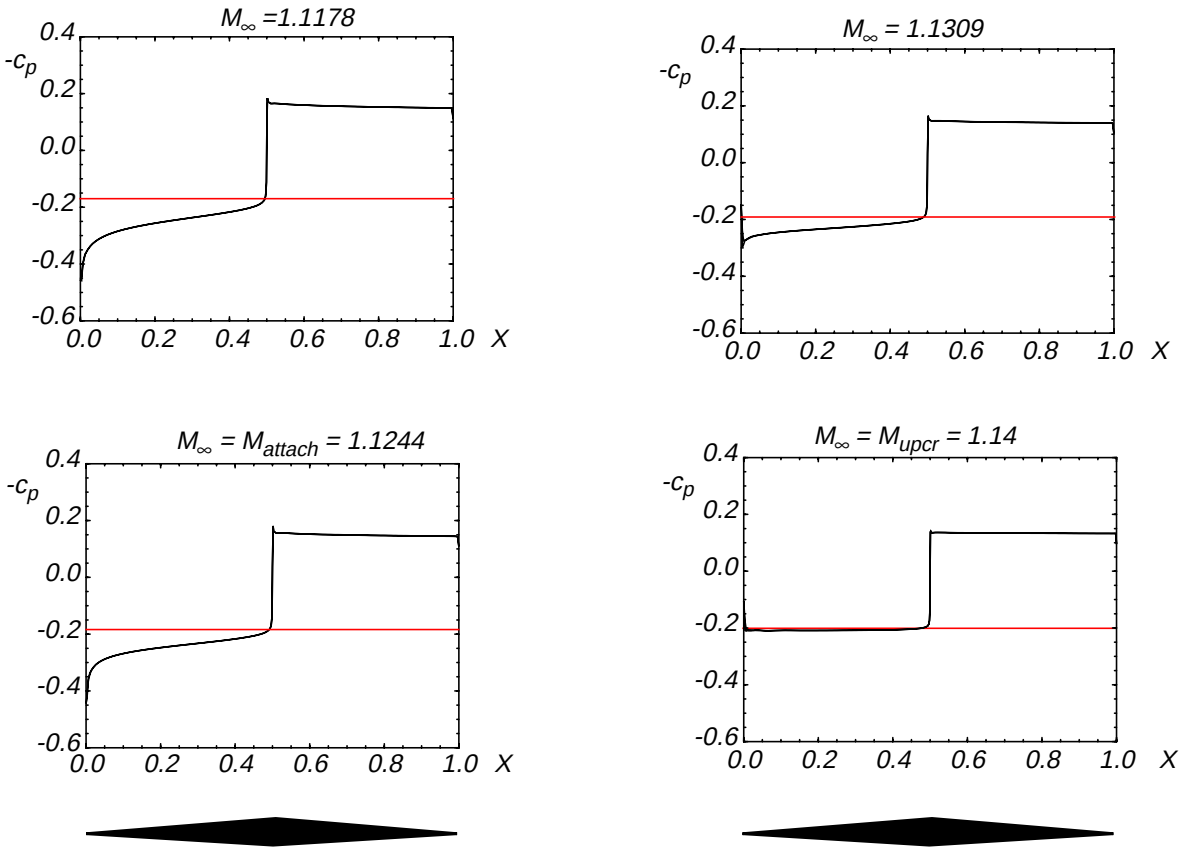

Figure 10. Pressure coefficient for diamond airfoil, different slightly supersonic Mach numbers: Observing leading edge singularity turning from stagnation point to logarithmic (at M_{attach}) and power expansion model, finally to regular supersonic wedge flow (at $M_\infty = M_{upcr}$)

CONCLUSION

A selection of exact solutions to the basic inviscid transonic equations have been used to define test cases for numerical simulation as well as alert the designer to special structures of possible target functions for inverse design and optimization: Locally singular behavior modelling might be needed to define well-posed boundary conditions in near sonic flow conditions.
Increasing importance of refined flow control brings back earlier idealized flows: mechanical control devices like for variable camber may allow for control surfaces improving leading edge flow quality and overall aerodynamic performance.
Incorporation of the presented exact solutions in general surface definition preprocessing codes as well as in target function generators will include these models in the manifold of configurations which inverse design might achieve and which a genetic optimization strategy might select to be among results with an improved fitness function.

REFERENCES

1. National Aerospace Laboratory (Ed): Proc. International Workshop on Numerical Simulation Technology for Design of Next Generation Supersonic Transport. Tokyo, 17-19 Jan. 2000.
2. Sobieczky, H.: Tragende Schnabelprofile in stossfreier Schallanströmung, Zeitschrift für angewandte Mathematik und Physik (ZAMP), Vol. 26, pp.819-830 (1975)
3. Sobieczky, H.: On Conical Flow (invited). 2nd AIAA Theoretical Fluid Mechanics Conference, AIAA-98-2594 (1998)
4. Sobieczky, H.: Die Abgelöste Transsonische Kopfwelle. Zeitschr. Flugwiss. (ZfW), Vol. 22, No. 3, pp. 66-73 (1974)
5. Sobieczky, H.: Anlegen der Kopfwelle bei Schallnaher Überschallströmung. Max-Planck-Forschungspreis 1991 Techn. Note DLR IB 221-92 A 36, (1992)
6. Klein, M., Sobieczky, H.: Sensitivity of aerodynamic optimization to parameterized target functions. In: M. Tanaka, G.S. Dulikravich, (Eds.), Inverse Problems in Engineering Mechanics, Proc. Int. Symp. on Inverse Problems in Engineering Mechanics (ISIP2001), Nagano, Japan (2001)
7. Trenker, M., Geissler, W., Sobieczky, H.: Airfoils with Dynamic Transonic Flow Control. AIAA 00-4419, (2000)
8. Gerhold, T., Friedrich, O., Evans, J. (1997) Calculation of Complex Three-Dimensional Configurations Employing the DLR τ-Code, AIAA 97-0167 (1997)